COBEM 2021
26th International Congress of Mechanical Engineering
ABCM
Associação Brasileira de Engenharia e Ciências Mecânicas
November 22-26, 2021, Virtual Congress, Brazil

COBEM-2021-2246
AN EXPERIMENTAL STUDY ON GROUND INFLUENCE AT HORIZONTAL AXIS TURBINES

Guilherme Tabatinga Medeiros, guilherme.tab@gmail.com[1]
Reginaldo Nunes da Silva, profreginaldo.n@gmail.com[1]
Rafael Castilho Faria Mendes, rafael.cfmendes@gmail.com[1]
Taygoara Felamingo de Oliveira, taygoara@unb.br[1]
Antonio Cesar Pinho Brasil Junior, brasiljr@unb.br[1]
[1]Universidade de Brasília. Faculdade de Tecnologia. Laboratório de Energia e Ambiente. 70910-900 Brasília-DF BRASIL

Abstract. *In turbulent horizontal axis turbine flows, it is necessary to understand the influence of the terrain on the generation of flow structures, where ground roughness is a crucial variable in rotor efficiency, such as hydrokinetic turbines placed in shallow rivers. Thus, this work presents an experimental study on the influence of the ground on the wake close to the horizontal axis turbines, seeking to describe the rotor mat, which is characterized by a complex system of coupled vortices, with high heterogeneity and turbulence instability. The wind tunnel experiments were carried out on a 1.2x1.2 m test section for a 4-blade horizontal axis turbine based on the NACA4412 profile with a diameter of 230 mm. Hot-wire anemometry was used to measure the mean longitudinal velocity profile for two experimental setups, with and without roughness. Wakes regions with high vorticity were identified the helical tip vortex signatures were identified where it is more intense at the height of the upper tip of the blade for both cases. It was also observed that roughness influences the energy available at rotor frequencies because with roughness the energy is presented in F/Ft=1, which shows that roughness accelerates the recovery of the turbine wake.*

Keywords: *Near-wake, HAWT, Turbulence, Hotwire Anemometry, Roughness.*

1. INTRODUCTION

Even with the significant developments in the aerodynamic design of horizontal axis wind turbines, the interactions in the turbine wake still have knowledge gaps due to their complexity and highly turbulent phenomena, but when studied and understood it is possible to extract important characteristics for the construction of wind projects. Detailed information about turbine wake properties, including medium flow characteristics and turbulence structures, is of great importance to optimize turbine location, maximize energy production (Zhang *et al.*, 2013). Horizontal axis turbine mats are characterized by complex turbulent flow structures with rotational movement induced by the turbine blades, with longitudinal and radial pressure gradients, and spiral vortices originating from tip vortices launched by the blades (Chamorro and Porté-Agel, 2009).

In wind turbine and hydrokinetic turbine rotor designs, there are two characteristics to be observed in turbine wakes that are of considerable practical interest: energy deficit, which is associated with the loss of energy from the turbine; and turbulence levels, which can affect rotor loads induced by flow in other turbines located downwind, or even by ground roughness upstream of the rotor (Vermeer *et al.*, 2003; Chamorro and Porté-Agel, 2009; Gaurier *et al.*, 2020). It is noteworthy that the energy conversion by the wind turbine is carried out by the same principles as the hydrokinetic turbine, however, the physical essence of the flow is different, in which, according to Myers and Bahaj (2010), the hydrokinetic flow is more regular and predictable due to the nature of the water currents. In fact, the contrast between the size of the turbines and their flows can be highlighted.

To understand these effects, scale models can be used. For hydrokinetic turbines, for example, scale arguments demonstrate that it is possible to obtain dimensionless performance parameters under a set of similarity conditions (geometric, kinematic and dynamic) using airflow and, finally, transpose model results to scale the actual prototype in water flow (Macias *et al.*, 2014). In scale experiments carried out, it was concluded that for horizontal axis hydrokinetic turbines, for a low tip speed (TSR), rotors with more than three blades are suitable for the performance of the turbine and also for the torque characteristics, necessary in the start-up operation regime (Brasil Junior *et al.*, 2019). In this paper, a 4-blade turbine was used.

Through a characterization of hydrokinetic turbines belt carried out by Britto *et al.* (2018), it was observed that the turbulence intensity is concentrated in the regions posterior to the rotors, where they have a characteristic of growing in half the diameter and then decreasing with distance. Researches indicate that the positioning of the horizontal axis wind turbine is within the atmospheric boundary layer, suffering influences from the ground. Something similar can be observed for the horizontal axis hydrokinetic turbines, which can be positioned in shallow rivers due to the boundary conditions in the design, in which it is possible that the turbine wake is influenced by the ground. The smooth surface allows a laminar flow inlet, which can be used as a reference.

In a detailed analysis carried out by Neunaber *et al.* (2020), In a detailed analysis carried out by JOAO, four downstream wake regions were revealed whose extension depends on the inflow turbulence, which could be identified in all scenarios through an investigation of the centerline only, through the average velocity, variance, turbulence intensity, energy spectrum, integral scales and other parameters. In a research carried out by Chamorro and Porté-Agel (2009), in which the interaction of the ground with the turbine mat for rough and smooth surfaces was studied, a non-axisymmetric wake of the mat was observed in both types of roughness in response to the non-uniform flow inlet of the boundary layer and surface effects. For these same profiles, the velocity deficit relative to the arrival velocity profile is almost axisymmetric, except near the ground in the distant wake, where the wake interacts with the surface. It was observed in this study that the axial non-symmetry of the distribution of the turbulence intensity of the wake is considered high on the rough surface, where the inflow is less uniform at the level of the turbine.

With the need to understand the interactions that the ground can exert on horizontal axis turbines wake, in this paper, the effect of boundary layer flow on the characteristics of the conveyor wake close to the turbine was studied using precise measurements in a wind tunnel. Emphasis is placed on the study of the distribution of mean wind speed in the direction of flow (and corresponding velocity deficit) and turbulence intensity in a plane parallel to the turbine flow in the direction of the inlet velocity. Considering the flow direction as the X-axis, the transverse direction perpendicular to the wake axis horizontally as the Y-axis and the direction perpendicular to the turbine axis vertically, treated as the direction of the height of the tunnel cross-section, as the Z-axis. The experiments were carried out under conditions of stability on a rough and smooth surface, in order to study the effect of roughness and the resulting mean flow. The experimental set-up is presented in section 2. The results obtained and the discussion are in section 3, in which the spatial distribution of the flow statistics measured in the neighboring regions and analyzed for two types of ground is presented. A conclusion summarizing the main points of the study is in topic 4.

2. EXPERIMENTAL SET-UP

2.1 Wind Tunnel - LEA-UnB

The experiments were carried out in the open-circuit wind tunnel at the Energy and Environment Laboratory of the University of Brasília, shown in Fig. 1. The test section for study development has a length of 2 meters and a cross-section of 1.2 x 1.2 m^2, an axial fan located at the exit of the tunnel generates a flow with a velocity ranging from 0 to 20 m/s and with turbulence intensity in the free flow of less than 1%. The tunnel is instrumented with a Pitot tube connected to a manometer (shown in details of Figs. 2(a) and 2(b)) for speed control and a temperature sensor.

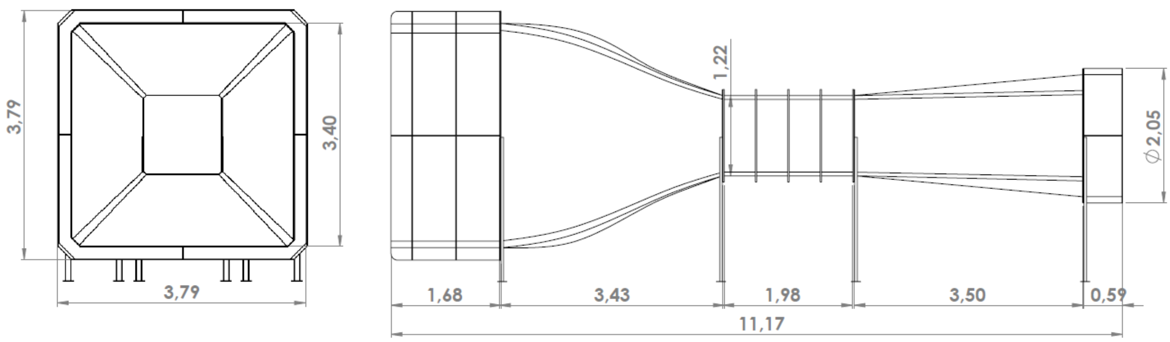

Figure 1. Image of the Energy and Environment Laboratory wind tunnel.

2.2 Turbine Scale Model

The experiments were carried out with a 1:10 scaled turbine, with four blades and based on a NACA4412 profile with 230 mm in diameter, manufactured using the additive manufacturing technique, using 3D printing of the rotor, presented Mendes (2020). It is common to use the blade tip speed λ in the study of turbines. This dimensionless value relates the tangential velocity at the tip of the blade with the undisturbed flow velocity upstream, and for the turbine used in this paper, the power coefficient curve was characterized and an average λ of 1.65 was calculated for one rotor rotation. 1000

(a) Pitot tube. (b) Differential pressure gauge.

Figure 2. Sensors used for wind tunnel speed control (Mendes (2020)).

rpm in a constant Reynolds number condition. A 240 mm tall tower was used to assemble the turbine rotor which, in addition to being a structural support, is also responsible for integrating the generator and all sensors, the model is shown in Fig. 3.

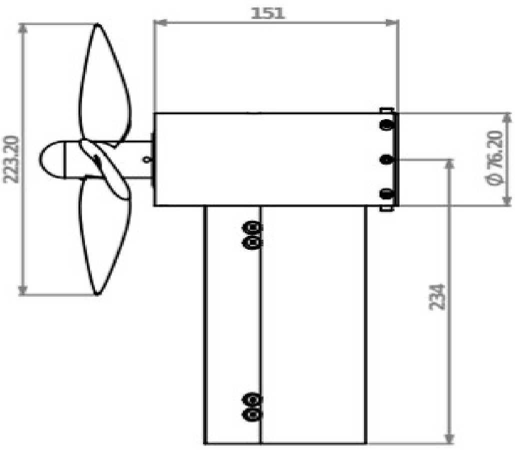

Figure 3. 1:10 scale model of the turbine used in the experiment, dimensions in millimeters (Mendes (2020))

The model has a TCRT5000 optical sensor (Fig. 4(b)) for the detection of the passage of the blade passage, composed of four reflective flaps, shown in the Fig. 4(a). More details about this system can be found in Mendes (2020).

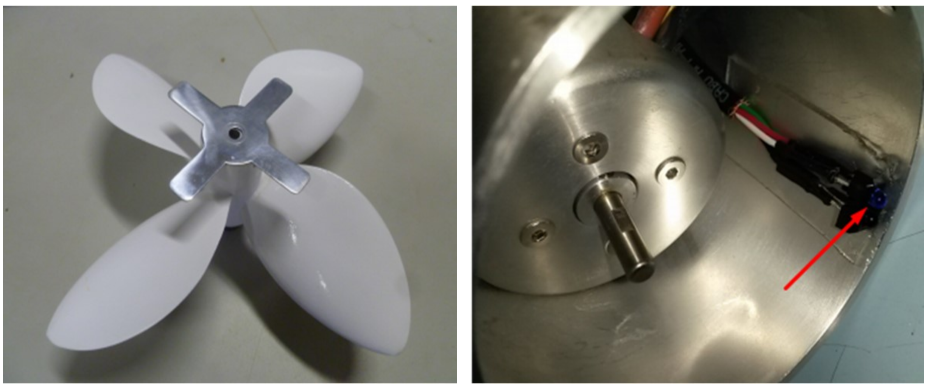

(a) Disc with reflective blades. (b) TCRT5000 optical sensor.

Figure 4. System for measuring turbine rotation (Mendes (2020))

The turbine was subjected to a flow at a velocity $U_\infty = 7,5m/s$, and a rotor rotation controlled at 1000 rpm, for the two cases presented in Figs. 5(a) and 5(b), and through automated hot-wire anemometry, Fig. 6(a), it was velocity acquisition was performed in the XZ plane shown in figure 6(b), for an increment of dx = 20mm and dz = 10mm.

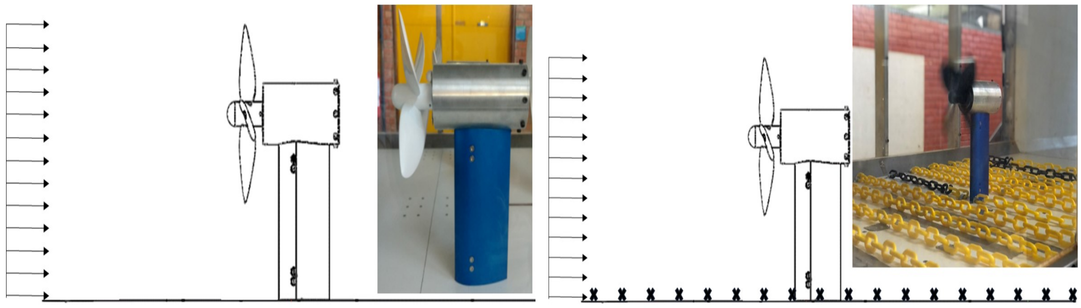

(a) Experiment without roughness. (b) Roughness experiment.

Figure 5. Experimental Settings.

2.3 Velocity data acquisition

Velocity data acquisition is performed by a hot wire anemometer probe. The probe is fixed in a positioner with displacement in the X, Y and Z axes, as illustrated in the Fig. 6(a). The control of the displacer is through stepper motors, being carried out by an electronic circuit implemented together with an Arduino board. According to Mendes (2020) the spatial precision of the system is 0.1 mm.

The acquisition plan was defined at 50% dof the turbine blade orthogonal to the Y axis, illustrated in Fig. 6(b), in which Chamorro and Porté-Agel (2009) found kinetic energy effects of greater intensity.

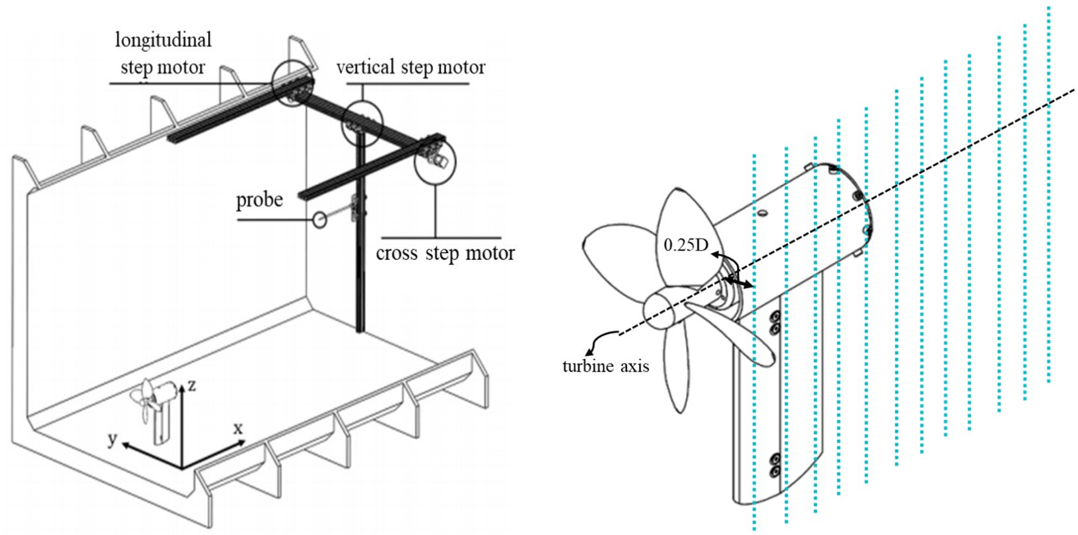

(a) Probe Positioning System in Wind Tunnel Test Section (Mendes (2020)). (b) Speed data acquisition plan, adapted from Mendes (2020).

Figure 6. Velocity data acquisition system.

Every system is controlled through proprietary code developed in MATLAB. The anemometer used is a mini-CTA 54T42 DANTEC model, connected to a 12-bit National Instruments DAQ-CARD 6062e acquisition board, varying the voltage from -10 to 10 volts. The components of a hot-wire anemometer system are shown in Fig. 7.

The anemometric probe is connected to a hot wire Wheatstone bridge through a feedback system and this performs the measurement of the current variation during the experiment. The bridge connects to the signal conditioner for signal amplification and noise elimination. The signal is sent to an analog-to-digital converter that converts the analog signal into digital, allowing data acquisition.

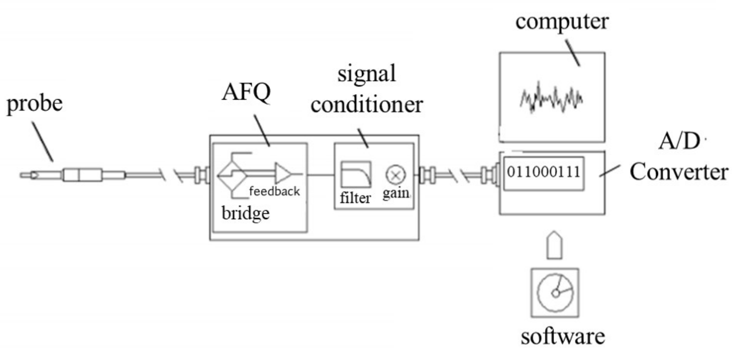

Figure 7. Schematic of hot wire anemometer components, adapted from Jørgensen (2002).

3. WAKE CHARACTERISTICS

3.1 MEAN VELOCITY

A detailed longitudinal characterization of the turbine wakes in the wind tunnel, over the rough and smooth surfaces, was obtained from high-resolution single probe hot-wire anemometry measurements collected at different positions in the flow direction. Velocity measurements were performed in the XZ to Y plane at a distance from the turbine axis of 25% of the blade diameter. In Figure 8 it is possible to observe the velocity contour for the smooth ground (Fig. 8(a)) and the ground rough (Fig. 8(b)) downstream of the turbine. For this value of Y, it was observed that, from X/D = 0 to X/D = 2.55, it shows an almost symmetrical behavior of the average velocity for the case that has roughness, and the same can be observed in the turbulence intensity in the Fig. 10(b).

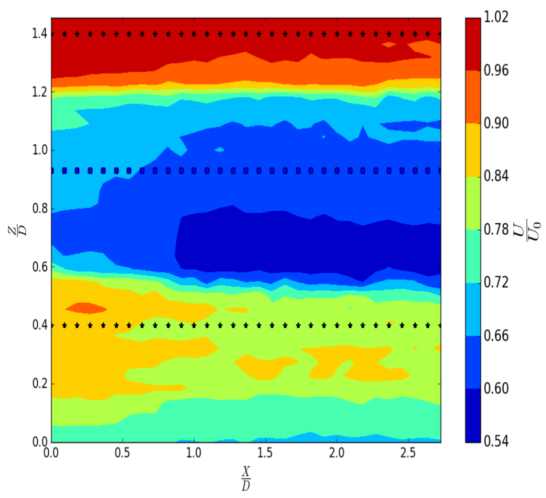

(a) Smooth surface.

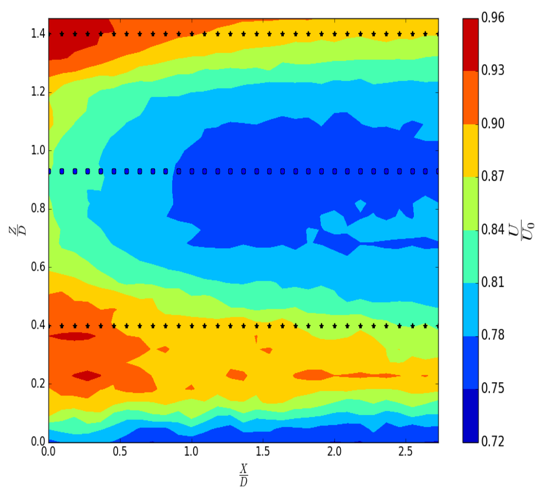

(b) Rough surface.

Figure 8. Turbine downstream speed contour. Dimensionless with $\frac{U}{U_0}$, the central dotted line indicates the axis of the turbine, and the other two are the position of the upper and lower blade tips.

Analyzing the velocity profiles of the wake close to the turbine, Fig. 9(a), it can be observed a reduction in velocity, modulated by the turbine, more intense in the case with smooth surface than in the case with rough surface. The velocity deficit calculated with respect to the inlet sounding velocity distribution is non-symmetric with respect to the axis of symmetry located slightly above the height of the rotor hub on the smooth surface. Part of this asymmetry is associated with the size of the turbine nacelle, which has a diameter 2.5 times larger than the diameter of the rotor hub. This difference in diameter totally changes the behavior of the turbine wake core due to the interaction between the helical vortices formed at the tip of the rotor blade and the turbine nacelle. In the range of Z/D = 0 to Z/D = 0.4, where a velocity deficit can also be perceived, the drop in magnitude is mainly associated with the encounter of turbulent flows by the wake at the lower end and the growth of the boundary layer on the surface.

Analyzing the profiles and the velocity deficit, Fig. 9(b),Analyzing the profiles and the velocity deficit, Fig. 9(b), we observe that in the short wake (X/D = 0 a X/D = 2.55), nat points above the height of the upper blade tip, in the flow without roughness , the treadmill has velocity with values in deficit less than 5% n relation to the entrance speed, being practically free flow. Just below, exactly at the height of the upper blade tip, the helical blade tip vortex signature is identified, and the velocity deficit reaches 30% of the free flow velocity and decelerates with the behavior of a conforming first-order function it goes down to the lower blade tip, which reaches a little more than 40% in cases equal to or greater than X/D = 1. At Z/D = 0.6 we have a partial recovery of the flow, but it returns to an increasing velocity deficit in the first-order up to the boundary layer, showing us that part of the nearby flow there is turbulence that influences the deceleration of the free flow.

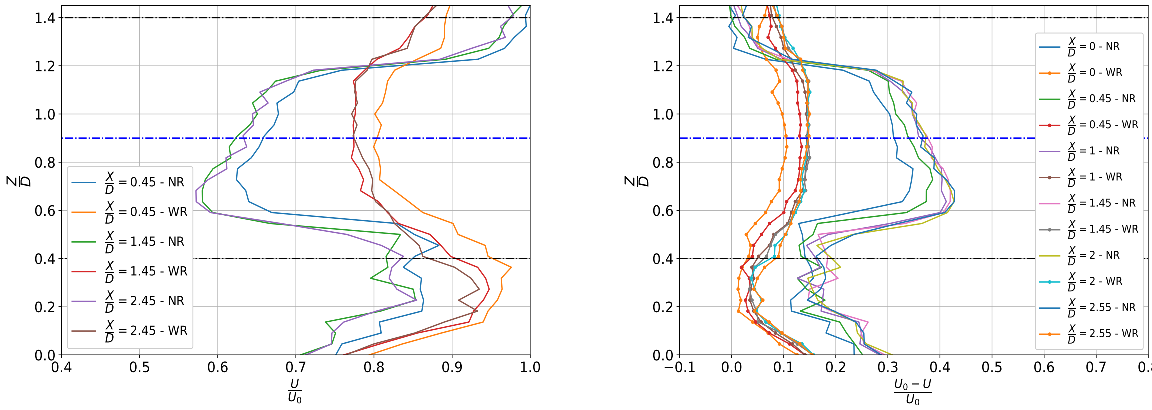

(a) (b)

Figure 9. (a) Velocity profile along $\frac{X}{D}$ com e sem rugosidade (b) Velocity deficit (NR - Without roughness and WR - With roughness).

In the flow with rough surface, a similar velocity deficit behavior is observed for the same points in relation to the smooth surface, but the velocity reaches at most a difference of 15% of the free flow, and in the height range between the tips of the blades, the deficit is characterized as a second-order function. In the rough case, in relation to the one without roughness, the ones closest to the surface present the biggest decelerations, indicating a considerable influence of the ground. Interestingly, the presence of a rough surface contributed to a faster recovery of the turbine wake.

3.2 TURBULENCE INTENSITY

To estimate the addition of turbulence intensity I_+, Eq. (1) is being defined as a function of the turbulence intensity of the flow before the turbine I_0 and the turbulence intensity in the wake $I_{Esteira}$, in which the turbulence intensity is obtained from the dimensioning of the square root of the variance, that is, the coefficient of variation of the probability density function for a turbulent variable U, Eq. (2).

$$I_+ = \sqrt{{I_{wake}}^2 - {I_0}^2} \tag{1}$$

$$I = \frac{\sigma_U}{\overline{U}} = \frac{\sqrt{\frac{1}{N-1}\sum_{i=1}^{N} U_i'^2}}{\overline{U}} \tag{2}$$

Regarding turbulence, it is expected that in the nearby belt ($X/D \leq 5$) it is expected to find a peak in turbulence intensity around the turbine belt tip, associated with the high turbulence levels produced by the helical vortex that they derive of the turbine blade tip vortices Hahm and Wußow (2006). In Figs. 10 e 11 are presented the addition profiles of turbulence intensity I_+ and the spatial distribution of turbulence intensity, both for the condition of $\lambda_{1,65}$, respectively. The turbulence intensity decreases in the lower wake region due to the reduction in average shear and turbulence kinetic energy production in relation to the inflow, in which this effect is more noticeable in the rough case. The turbine effect was expected to lead to an increase in the turbine wake compared to the intensity of inflow turbulence, which can lead to increased fatigue loads on other wind turbines located downwind in a park wind power.

Comparing the turbulence intensity distributions of Fig. 9, it can be observed that in the roughest case there is a degree of non-axial symmetry of the turbine wake and its evolution, which for the region close to the belt can be concluded that there is a diffusive transport through turbulent dissipations. The wake on the smooth surface shows a relatively smaller deviation from the axis symmetry compared to the case of the rough surface, even when it hits the surface. This can be explained considering that the inlet velocity field is more uniform compared to the rough case, in which the more uniform

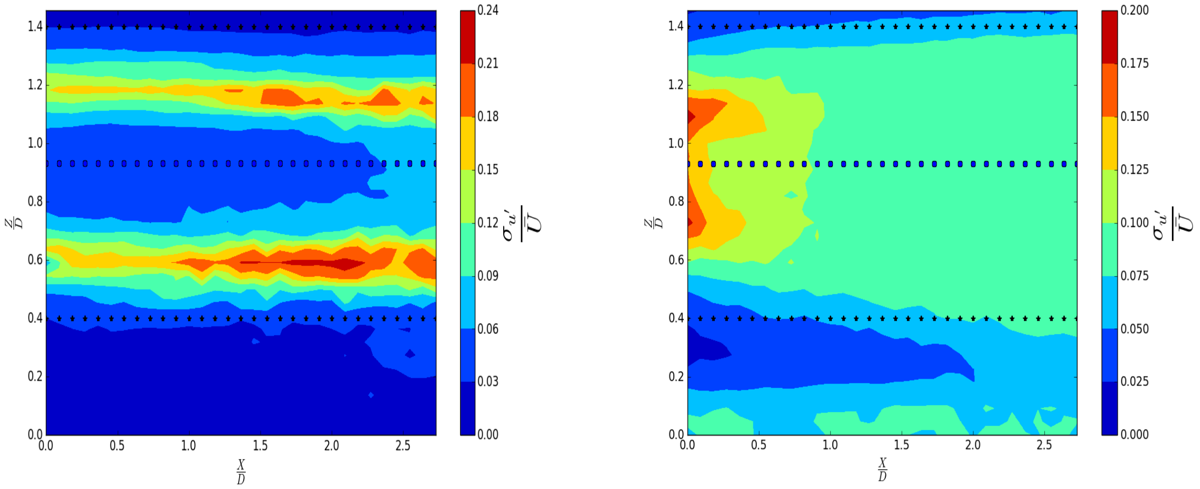

(a) Smooth surface. (b) Rough surface.

Figure 10. Spatial distribution turbulence intensity downstream of the turbine.

the inlet flow at the turbine level, the smaller the deviation of the belt axis symmetry. In the limiting case of a uniform inflow (for example, a turbine placed in a free-flowing stream), the turbine wake is axisymmetric Hahm and Wußow (2006). Although axisymmetry is not obtained in rough flow, the diffusion of turbulence intensity that occurs in this case can contribute to the recovery of the turbine mat in a smaller longitudinal distance in the direction of flow in relation to the case of smooth surface.

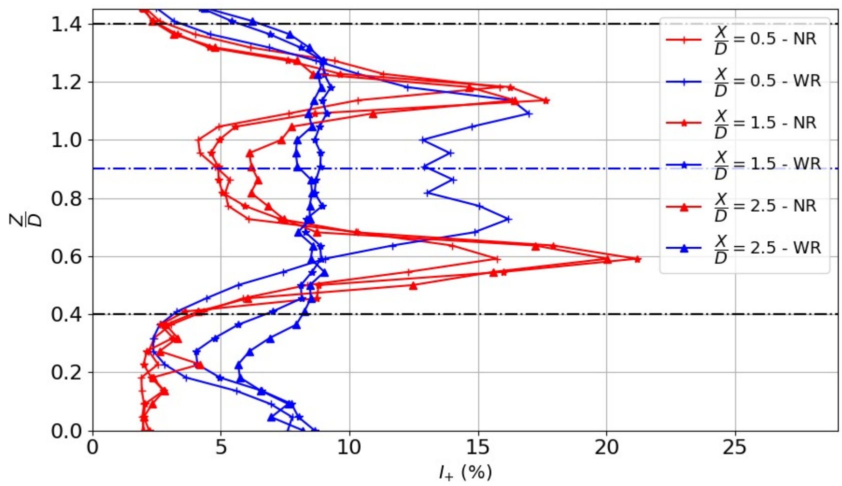

Figure 11. Turbulence intensity for different points in $\frac{X}{D}$

3.3 KINETIC ENERGY

The Fourier transform of the autocorrelation function is called as a power spectrum density and is defined by,

$$(u'_t u'_{t+\tau})/\sigma_u{}^2 = \int_{-\infty}^{\infty} e^{i\tau\omega} S(\omega) d\omega \tag{3}$$

$$S(\omega) = \frac{1}{2\pi} \int_{-\infty}^{\infty} e^{-i\tau\omega} (u'_t u'_{t+\tau})/\sigma_u{}^2 d\tau \tag{4}$$

The Equations (3) e (4) define the Fourier transform pair, where ω is the angular velocity of the phase, the i represents the complex term, τ is the integral time scale.

The Figure 12 shows the spatial distribution of the kinematic shear stress for the different measurement locations. From this figure, it is clear that the turbine introduces kinematic stresses that are locally much greater in magnitude than the tension in the input velocity field. In the region of the nearby wake, at the distances $X/D \leq 5$, there is a region above the turbine hub and below it with a high concentration of energy. As in the case of velocity deficit and turbulence intensity, the change in kinematic tension in relation to the input flow remains non-negligible. It is evident that asymmetry of the incoming wind can reduce or increase average power generation, depending on the sign of the asymmetry coefficient, just as Chamorro and Porté-Agel (2009) noted.

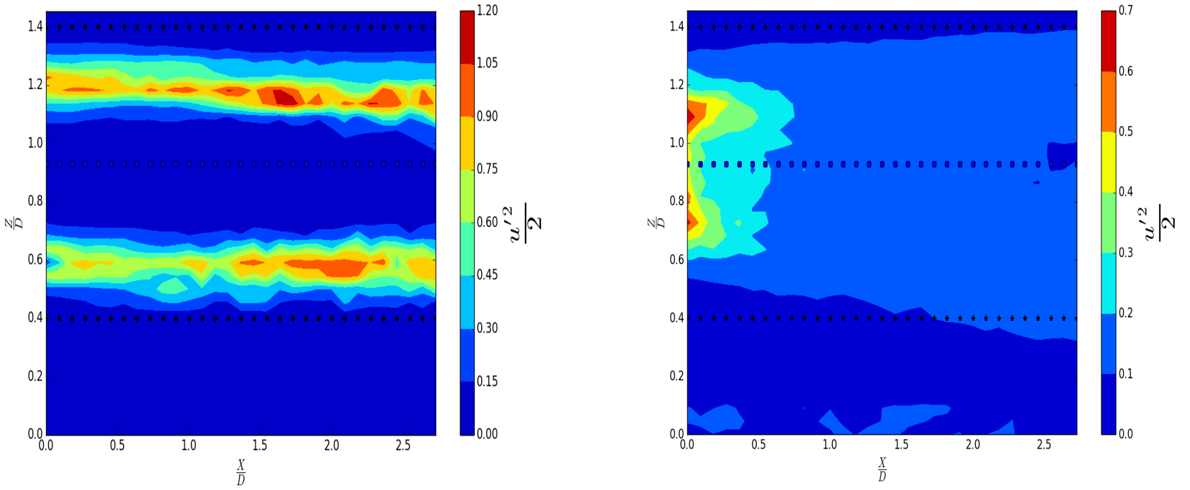

(a) Smooth surface. (b) Rough surface.

Figure 12. Spatial distribution of turbulent kinetic energy downstream of the turbine.

An analysis for the spectral domain was performed in order to identify the energetic contributions of different frequencies present in the turbulent flow to the wake flow of the turbine model, which can be seen in Fig. 13. As the graph of this figure is dimensionless according to the rotor rotation frequency, for $X/D = 1$ we can conclude that both in the case without roughness and in the case with roughness there is a concentration of the power spectral density (PSD) with the biggest peak exactly at the turbine rotation frequency, which was expected according to Chamorro and Porté-Agel (2009).

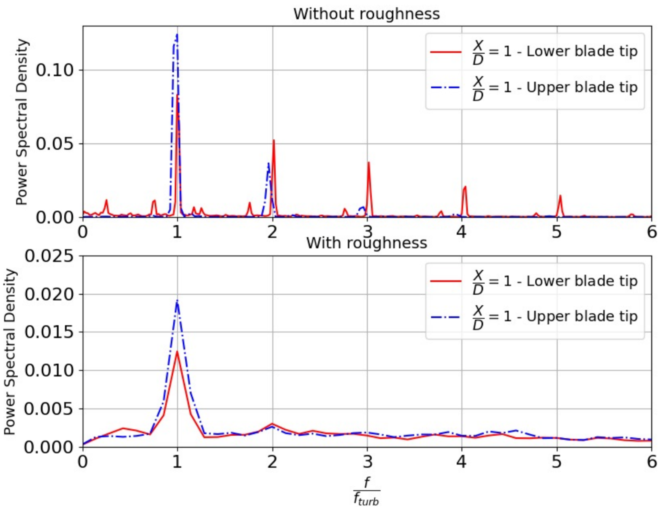

Figure 13. Power Spectral Density.

It is noticeable that the power spectral density distributions have the highest values in the upper blade tip than in the lower one, for both surfaces, which would be expected due to what was analyzed in the velocity deficit. Furthermore, a damping phenomenon due to roughness occurs on the non-smooth surface, in which, in the diffusion process, the dominant frequency, which is the same as the rotor at $\lambda_{1,65}$, has the highest density peaks and for the other frequencies it is almost normalized, unlike the smooth surface, which for several harmonics still has considerable density peaks. In this case, it is evident that, with the rough surface, the recovery of the wake takes place more quickly than on the smooth surface, caused by the diffusive phenomena that occur due to the ground.

4. SUMMARY

In order to study the effects of boundary layer turbulence and surface roughness on the downwind conveyor structure of a horizontal axis turbine model, an experiment was carried out in a wind tunnel. Automated single probe hot wire anemometry within the wind tunnel was used to obtain detailed measurements of wind speed, turbulence intensity and kinetic energy in a longitudinal section located at 50% relative to the axis of the turbine horizontally, in the XZ plane in the direction of the inlet flow. The velocity deficit in the profiles was calculated for different distances in X in relation to the blade diameter, in order to obtain a better understanding of the turbulence inside the wake. The positioning of the turbine within the wind tunnel was limited to a cross-sectional area of $1,2x1,2m$ and $2m$ longitudinal length parallel to the flow, in which it was placed in a boundary layer developed over rough surfaces and smooth under equal conditions. The experiments were carried out with a 1:10 scaled turbine, with four blades and based on a NACA4412 profile $230mm$ in diameter and a fixed shaft height, in relation to the tunnel surface, of $240mm$ height. Emphasis was placed on quantifying the magnitude of the velocity deficit and increasing the turbulence intensity in the turbine wake in relation to the boundary layer inflow.

The arrangement of the inflow of the boundary layer, which is modulated by the surface, influences the distribution of turbulence properties within the turbine belt was observed. It was observed that, from x/d = 0 to x/d = 2.5, it shows an almost symmetrical behavior of the mean velocity for the case that has roughness, and the same can be observed in the turbulence intensity. A more intense reduction of the velocity can be observed in the case with a smooth surface than in the case with a rough surface. The velocity deficit calculated with respect to the incoming wind speed distribution is non-symmetric with respect to the axis of symmetry located slightly above the height of the engine hub on the smooth surface. A velocity deficit associated mainly with the encounter of turbulent flows by the flow from the mat at the lower end and the growth of the boundary layer near the surface for both types of ground was observed. For the smooth surface, between the blades, a deficit of 30% was obtained at the top and a constant deceleration up to 40% at the bottom was obtained. In the case with roughness, a similar velocity deficit behavior was observed for the same points in relation to the smooth surface, but the velocity reaches at most a difference of 15% of the free flow and with a deceleration characterized as a function of second order, that is, the presence of a rougher soil contributed to a shorter recovery in the longitudinal direction of the turbine wake.

It was compared the turbulence intensity distributions of the, it was observed that in the roughest case there is a degree of non-axial symmetry of the turbine mat and its evolution, that for the region close to the mat it can be concluded that there is a diffusive transport through dissipations turbulent. The wake on the smooth surface shows a relatively smaller deviation of axis symmetry compared to the rough surface case, even when it hits the surface, because the input velocity field is more uniform compared to the rough case, in which how much the more uniform the inflow at the turbine level, the less the deviation from the symmetry of the rotor axis. It was concluded that although axisymmetry is not obtained in rough flow, the diffusion of turbulence intensity that occurs in this case can contribute to the recovery of the turbine wake in the short wake.

For X/D = 1 we can conclude that both in the case without roughness and in the case with roughness there is a power spectral density (PSD) concentration with the highest peak exactly at the turbine rotation frequency. A damping phenomenon due to roughness occurs on the non-smooth surface, in which, in the diffusion process, the dominant frequency, which is the same as the rotor at $\lambda_{1.65}$, has the highest density peaks and for the other frequencies is almost normalized, unlike the smooth surface, which for various harmonics, has considerable density peaks. However, it was concluded that, with the rough surface, the recovery of the wake takes place more quickly than on the smooth surface, caused by the diffusive phenomena that occur due to the ground.

5. ACKNOWLEDGEMENTS

The authors would like to thank Serra do Facão Energia S.A. for providing financial support for the development of the project ($ANEEL : P\&D06899 - 2002/2020$) - *Desenvolvimento de metodologia para determinação de potencial de energia hidrocinética em usinas hidroelétricas.*

This authors was financed in part by the *Coordenação de Aperfeiçoamento de Pessoal de Nível Superior - Brasil* (CAPES) - Finance Code 001.

6. REFERENCES

Brasil Junior, A.C.P., Mendes, R.C.F., Wirrig, T., Noguera, R. and Oliveira, T.F., 2019. “On the design of propeller hydrokinetic turbines: the effect of the number of blades”. *Journal of the Brazilian Society of Mechanical Sciences and Engineering, Springer Verlag*, Vol. 41, No. 6, pp. 1–15.

Britto, V.S., Mendes, R.C.F., Brasil, A.C.P. and Oliveira, T.F., 2018. "Wake characterization in row array of hydrokinectics turbines". *Revista da Engenharia Térmica*, Vol. 17, No. 1, pp. 41–48.

Chamorro, L.P. and Porté-Agel, F., 2009. "A wind-tunnel investigation of wind-turbine wakes: Boundary-layer turbulence effects". *Boundary-Layer Meteorol*, Vol. 132, p. 129–149.

Gaurier, B., Ikhennicheu, M., Germain, G. and Druault, P., 2020. "Experimental study of bathymetry generated turbulence on tidal turbine behaviour". *Renewable Energy*, Vol. 156, pp. 1158–1170. doi: https://doi.org/10.1016/j.renene.2020.04.102.

Hahm, T. and Wußow, S., 2006. "Turbulent wakes in wind farm configuration". Vol. 2, pp. 1387–1394.

Jørgensen, F., 2002. "How to measure turbulence with hot-wire anemometers - a practical guide".

Macias, M.M., Mendes, R.C.F., Silva, P.A.S.F., Oliveira, T.F. and Junior, A.C.P.B., 2014. "A feasibility study on the use of wind tunnel experiments for hydrokinetic turbines". In *International Group for Hydraulic Efficiency Measurements - IGHEM 2014*. Itajubá, Brazil.

Mendes, R.C.F., 2020. *Interação entre esteiras aerodinâmicas de turbinas de eixo horizontal em arranjos (in Portuguese)*. Master's thesis, Tese (Doutorado em Ciências Mecânicas)—Universidade de Brasília, Brasília, Brasil.

Myers, L.E. and Bahaj, A.S., 2010. "Experimental analysis of the flow field around horizontal axis tidal turbines by use of scale mesh disk rotor simulators". *Ocean Engineering*, Vol. 37, No. 2, pp. 218–227. doi: https://doi.org/10.1016/j.oceaneng.2009.11.004.

Neunaber, I., Hölling, M., Stevens, R.J.A.M., Schepers, G. and Peinke, J., 2020. "Distinct turbulent regions in the wake of a wind turbine and their inflow-dependent locations: The creation of a wake map". *Energies*, Vol. 13, No. 20. ISSN 1996-1073. doi:10.3390/en13205392. URL `https://www.mdpi.com/1996-1073/13/20/5392`.

Vermeer, N., Sørensen, J. and Crespo, A., 2003. "Wind turbine wake aerodynamics". *Progress in Aerospace Sciences*, Vol. 39, No. 6, pp. 467–510.

Zhang, W., Markfort, C.D. and Porté-Agel, F., 2013. "Wind-turbine wakes in a convective boundary layer: A wind-tunnel study". *Boundary-Layer Meteorol*, Vol. 146, p. 161–179.